

HIP-2001-19/TH

Radions in a $\gamma\gamma$ collider ^{*}M. Chaichian^{a,b}, K. Huitu^a, A. Kobakhidze^{a,b} and Z.-H. Yu^{a,b}^aHelsinki Institute of Physics^bDepartment of Physics, University of Helsinki
P.O.Box 9, FIN-00014 Helsinki, Finland

ABSTRACT

We study the resonance production of radions via $\gamma\gamma$ fusion in the Randall-Sundrum model. We find that the cross section of the process in the $\gamma\gamma$ mode of a linear collider (LC) can be of similar size as in the e^+e^- collision mode, if the radion is heavy. We consider the possible curvature-Higgs mixing in the model, and we find that the mixing should be constrained in order to avoid an unphysical state. The process $\gamma\gamma \rightarrow \phi$ is the main source of radions at LC near the conformal limit. We consider both the decay modes of radion with curvature-Higgs mixing and without. Our results show that the radion with mass below 800 GeV could be detected at LC with any mixing parameter and vacuum expectation value of the radion around 1 TeV.

^{*}The authors thank the Academy of Finland (project number 163394 and 48787) for financial support.

1. Introduction

One of the most fascinating outcome of the recently proposed brane World scenarios [1, 2] is a possibility to probe quantum gravity and entire structure of space-time at high energy colliders. The main theoretical motivation behind these models is a solution to the familiar problem of the observed hierarchy of scales, such as $M_{EW}/M_P \ll 1$, where M_{EW} and M_P are the electroweak and Planck scales, respectively.

An interesting possibility has been proposed by Randall and Sundrum (RS) within the model with 5-dimensional AdS space-time compactified on a S^1/Z_2 orbifold with two 3-branes stucked at the orbifold fixed-points (see the first paper in [2]). The background geometry has been found to be non-factorizable with a warp factor in the metric being an exponentially decreasing function of the fifth compact coordinate. Such a geometry provides the localization of zero-mode graviton on a Planck brane and exponential hierarchy between mass scales as seen by observers on different branes. Thus, contrary to the proposal of ref. [1], even small distance between two branes, determined by the radius of extra dimension, can explain the large hierarchy between M_{EW} and M_P if the visible world is localized on a TeV brane.

The size of compact extra dimension is given by a vacuum expectation value (GeV) of a certain scalar field called modulus (radion). Usually the moduli have runaway VEVs. Thus, the radion stabilization (see *e.g.* [3, 4]) in [1, 2] is a rather crucial point not only for the desired explanation of the hierarchy problem but also for obtaining consistent 4-dimensional gravity and cosmology on the visible TeV brane. Remarkably, the stabilized radion in the RS model is typically lighter than the low-lying Kaluza-Klein modes of graviton [3, 5]. Thus the radion might be the first state accessible in the high-energy experiments and study of its collider phenomenology will be important in order to test the model.

Recently many works have discussed the phenomenology of radions [5, 6, 7, 8, 9]. We'll study in this paper a specific model with curvature-Higgs mixing [10, 11]. At the two-derivative level scalars and gravity are coupled in the visible brane,

$$S = -\xi \int d^4x \sqrt{-g_{vis}} R(g_{vis}) H^+ H, \quad (1)$$

where the Ricci scalar $R(g_{vis})$ corresponds to the induced four dimensional metric on the visible brane and H is the electroweak Higgs boson. This term will introduce mixing between radion and Higgs in RS model, and will modify the phenomenology of radion strongly when compared to the unmixed case [10]. Especially near the conformal limit, $\xi = 1/6$, radion coupling to the Standard Model fields W , Z and fermions will be strongly suppressed, while gluon and photon interactions with radion will be only partially suppressed [10]. As a result, detecting radion at a

Linear Collider (LC) directly in e^+e^- collision will become difficult and production of radion by $\gamma\gamma$ fusion will be significant.

With the advent of new collider techniques, highly coherent laser beams can be produced by back-scattering with high luminosity and efficiency at the e^+e^- colliders [12]. A $\gamma\gamma$ resonance can be probed over a wide mass region. Thus the $\gamma\gamma$ collisions can produce heavier radions than the corresponding e^+e^- collisions. Recently in [9] the radion production in $\gamma\gamma$ colliders without mixing of radion and Higgs was discussed.

In section 2, we will discuss the coupling of radion to SM fields in the case of the curvature-Higgs mixing. In section 3 the numerical results are presented. Possible experimental signals are considered in section 4, where the decay widths are presented. The conclusions are given in section 5 and some details of the expressions are listed in the appendix.

2. Couplings of radion to the SM fields

In RS model [2], the single extra dimension is compactified on a S^1/Z_2 orbifold with coordinate y , $y \in [-\pi, \pi]$. The metric in the model is given by¹

$$ds^2 = e^{-2kr_c|y|} \eta_{\mu\nu} dx^\mu dx^\nu - r_c^2 dy^2. \quad (2.1)$$

where $1/k$ is the AdS curvature radius.

Following Refs. [6, 10], we define a radion field as

$$\phi = \Lambda_\phi e^{-k\pi(T-r_c)} \quad (2.2)$$

where M_5 is the Planck scale of the fundamental 5-dimensional theory, and Λ_ϕ is the VEV of the radion. $\Lambda_\phi = \sqrt{24M_5^3/k} e^{-k\pi r_c}$, which can be of the order of TeV. Integrating out the fifth dimension, one obtains the four dimensional effective action as [6, 10]

$$S = \int d^4x \sqrt{-g} \left[\frac{2M_5^3}{k} \left(1 - \frac{\phi^2}{\Lambda_\phi^2} e^{-2k\pi r_c} \right) R + \frac{1}{2} \partial_\mu \phi \partial^\mu \phi - V(\phi) + \left(1 - \frac{\phi}{\Lambda_\phi} \right) T_\mu^\mu \right], \quad (2.3)$$

where $V(\phi)$ is the potential stabilizing the radion field.

We will concentrate on T_μ^μ terms which will couple to radion, as given in [10, 11],

$$T_\mu^{(1)\mu} = 6\xi v \square h - 3\xi v^2 / \Lambda_\phi \square \phi, \quad (2.4)$$

¹Strictly speaking, inclusion of the Higgs-curvature mixing term (1) may generally modify the background solution (2.1). Say, after the electroweak Higgs boson acquires a VEV, $H = \frac{1}{\sqrt{2}}(h(x) + v)$, the 4-dimensional induced curvature will also appear in the effective Lagrangian affecting the background solution (2.1) [13]. Here we will ignore such a complication.

$$T_\mu^{(2)\mu} = (6\xi - 1)\partial_\mu h \partial^\mu h + 6\xi h \square h + 2m_h^2 h^2 + m_{ij} \bar{\psi}_i \psi_j - M_V^2 V_{A\mu} V_A^\mu, \quad (2.5)$$

where v is the VEV of Higgs. We will neglect terms of stress-energy tensor containing three or more fields in this paper.

$T_\mu^{(1)\mu}$ term induces a kinematic mixing between Higgs and radion. After shifting $\phi \rightarrow \phi + \Lambda_\phi$, the Lagrangian containing bilinear terms of radion and Higgs is obtained as

$$\mathcal{L} = -\frac{1}{2}\phi[(1 - 6\xi\gamma^2)\square + m_\phi^2]\phi - \frac{1}{2}h(\square + m_h^2)h - \frac{6\xi v}{\Lambda_\phi}\phi\square h. \quad (2.6)$$

Here m_ϕ is a mass parameter in $V(\phi)$ and $\gamma = v/\Lambda_\phi$. After diagonalization, the fields should be redefined as

$$\phi = a\phi' + b h', \quad (2.7)$$

$$h = c\phi' + d h', \quad (2.8)$$

where $a = \cos\theta/Z$; $b = -\sin\theta/Z$; $c = \sin\theta - 6\xi\gamma/Z \cos\theta$ and $d = \cos\theta + 6\xi\gamma/Z \sin\theta$, with $Z^2 = 1 - 6\xi\gamma^2(1 + 6\xi)$ and the mixing angle θ is given by

$$\tan 2\theta = 12\xi\gamma Z \frac{m_h^2}{m_h^2(Z^2 - 36\xi^2\gamma^2) - m_\phi^2}. \quad (2.9)$$

Our results agree with those in Ref. [10] (with $\xi\gamma \ll 1$) and in Ref. [11]. From Eq. (2.7-8), we see clearly the constraints $-(1 + \sqrt{1 + 4/\gamma^2})/12 \leq \xi \leq (\sqrt{1 + 4/\gamma^2} - 1)/12$, just as in Ref. [11].

The new fields ϕ' and h' are mass eigenstates with masses

$$m_{\phi'}^2 = c^2 m_h^2 + a^2 m_\phi^2 \quad (2.10)$$

$$m_{h'}^2 = d^2 m_h^2 + b^2 m_\phi^2 \quad (2.11)$$

The interaction Lagrangian of ϕ and h with fermions and massive gauge bosons,

$$\mathcal{L} = -\frac{1}{v}(m_{ij} \bar{\psi}_i \psi_j - M_V^2 V_{A\mu} V_A^\mu) \left[h + \frac{v}{\Lambda_\phi} \phi \right] \quad (2.12)$$

can be transformed to the coupling of mass eigenstates ϕ' and h' to fermions and massive gauge bosons as

$$\mathcal{L} = -\frac{1}{\Lambda_\phi}(m_{ij} \bar{\psi}_i \psi_j - M_V^2 V_{A\mu} V_A^\mu) [a_{34} \frac{\Lambda_\phi}{v} h' + a_{12} \phi'], \quad (2.13)$$

where $a_{12} = a + c/\gamma$ and $a_{34} = d + b\gamma$. The coefficients a_{12} and a_{34} give directly the strength of the corresponding interaction when compared to the case with no mixing.

As pointed out in Ref. [10], a_{12} can be approximately zero in the conformal limit $m_h = 0, \xi = 1/6$ when $\Lambda_\phi \gg v$. Thus the associated production in $e^+e^- \rightarrow Z\phi'$ becomes inaccessible at conformal limit and other production mechanisms should be considered.

The coupling of the radion to two Higgs bosons depends on $V(\phi)$ and mixing of radion and Higgs. Neglecting the radion self-coupling in $V(\phi)$, we can get the vertex of $h'h'\phi'$ as

$$\begin{aligned} & \frac{1}{\Lambda_\phi} (2m_h^2 ad^2 h'^2 \phi' - ad^2 \phi' \partial_\mu h' \partial^\mu h' (1 - 6\xi) + 6\xi ad^2 (h' \square h') \phi' \\ & + 4m_h^2 bcd \phi' h'^2 - 2bcdh' \partial_\mu \phi' \partial^\mu h' (1 - 6\xi) + 6bcd\xi h' (\phi' \square h' + h' \square \phi')). \end{aligned} \quad (2.14)$$

In addition to the tree-level T_μ^μ , there is also a trace anomaly term for gauge fields [14]. The effective vertex is given by

$$[(\frac{1}{\Lambda_\phi} (ab_3 - \frac{1}{2}a_{12}F_{1/2}(\tau_t))\phi' + \frac{1}{v}(\frac{v}{\Lambda_\phi}bb_3 - 1/2a_{34}F_{1/2}(\tau_t))h') \frac{\alpha_s}{8\pi} G_{\mu\nu}^a G^{\mu\nu a}] \quad (2.15)$$

for radion to gluons and

$$[(\frac{1}{\Lambda_\phi} (a(b_2 + b_Y) - a_{12}(F_1(\tau_W) + \frac{4}{3}F_{1/2}(\tau_t))\phi' + \frac{1}{v}(\frac{v}{\Lambda_\phi}b(b_2 + b_Y) - a_{34}(F_1(\tau_W) + \frac{4}{3}F_{1/2}(\tau_t))h') \frac{\alpha_{EM}}{8\pi} F_{\mu\nu} F^{\mu\nu}] \quad (2.16)$$

for radion to two photons, where $b_3 = 7$ is the QCD β -function coefficient and $b_2 = 19/6, b_Y = -41/6$ are $SU(2) \times U(1)_Y$ β -function coefficients in the SM. F_1 and $F_{1/2}$ are form factor from loop effects, which will be given in detail in appendix. We can see from Eq.(2.14,15) that the vertex can remain nonvanishing in the conformal limit. There will be significant terms when we consider physics near the conformal limit.

3. Radion production

The radion production cross sections via $\gamma\gamma$ fusion will be given in this section. When the mixing becomes strong, it will become less clear which is Higgs and which is radion. Since the mixing matrix of radion and Higgs is not unitary, we will always consider ϕ' as radion and h' as Higgs in the following calculations.

In Fig.1, we show the cross section of $\gamma\gamma \rightarrow \phi'$ as a function of the mass of radion $m_{\phi'}$ at c.m. energy $\sqrt{s}=500$ GeV, 700 GeV, and 1 TeV, respectively. In Fig. 1 radion is not mixed with Higgs, *i.e.* we set $\xi = 0$, $m_h = 150$ GeV, and $\Lambda_\phi = 1$ TeV. Compared with the results of Ref. [8], where the cross section of radion production from e^+e^- mode at a Linear Collider (LC) is considered, we find that the cross sections for heavy radions (with mass above 500 GeV) are of similar magnitude. The process should be considered as an important way to produce radions at LC, when there is no mixing. Our calculations agree with the results of Ref. [9] for this case.

In Figs. 2 (a) and (b), we plot the cross section of $\gamma\gamma \rightarrow \phi'$ as a function of the mass of the radion, $m_{\phi'}$, at c.m. energy $\sqrt{s}=500$ GeV, 700 GeV, and 1 TeV, respectively, when radion and Higgs are mixed, $\xi = 1/6$. ² The other parameters are set to $m_h = 150$ GeV, and $\Lambda_\phi = 1$

² The gap in the Fig.2 for $m_{\phi'}$ between 130 GeV to 190 GeV in Fig. 2 is due to the discontinuity in a^2 and c^2 in Eq.(2.10).

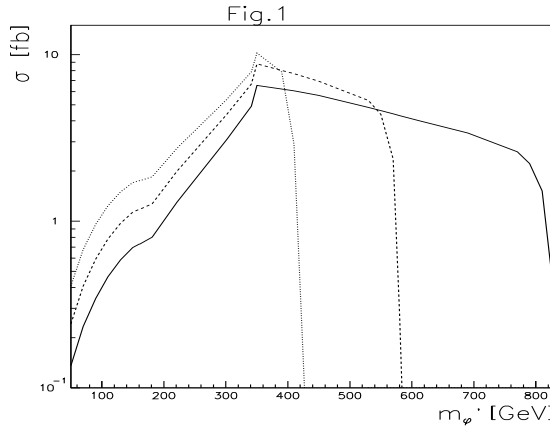


Figure 1: The cross section of $\gamma\gamma \rightarrow \phi'$ as a function of $m_{\phi'}$ with $\Lambda_\phi = 1$ TeV, $m_h = 150$ GeV and $\xi = 0$. The solid line corresponds to the center of mass energy 1 Tev, the dashed line to 700 GeV and the dotted line to 500 GeV.

TeV. We see from Figs. 2 (a) and (b) that there is an enhancement when $m_{\phi'}$ is near m_h and a suppression when $m_{\phi'}$ is much heavier than m_h . In Fig. 2 (c) and (d), we plot the cross section with otherwise the same parameters, but with $\Lambda_\phi = 10$ TeV. We find similar enhancement and suppression than in Figs. 2 (a) and (b), but much stronger. That is reasonable because mixing with Higgs will effect radion stronger with raising of Λ_ϕ/v .

In order to compare with the possible suppression and enhancement of mixing in e^+e^- collision, we draw the parameter a_{12} of Eq. 2.12 as a function of $m_{\phi'}$ for $\xi = 1/6, m_h = 150$ GeV and $\Lambda_\phi = 1$ TeV and 10 TeV, respectively, in Fig. 3 (a) and (b). Compared with [8], the cross section from e^+e^- collision is in our case smaller by a factor of 10^{-4} for radions heavier than 500 GeV but larger by two orders of magnitude for radions with mass m_h .

Therefore, for light radions, the production cross section in e^+e^- collisions is larger than in $\gamma\gamma$ collisions, while for heavy radion at conformal limit the situation is the opposite. Thus we can observe the radion with mass larger than 500 GeV (up to 800 GeV) with $\gamma\gamma$ collisions at LC with Λ_ϕ about 1 TeV (corresponding to hundreds of events with luminosity about 500 fb^{-1}), and for a light radion e^+e^- collision can scan it around the conformal limit.

To consider a general ξ , we draw a_{12} as a function of ξ in Fig. 3 (c) with $m_h = 150$ GeV and $m_{\phi'} = 100$ GeV and 800 GeV, respectively. We find that around the conformal limit, in the region about $0.1 < \xi < 0.2$, there will be suppression effects stronger than one order from mixing for heavy radions, while away from the region, effects will weaken and change to enhancement effects. For a light radion the interaction with fermions and gauge bosons is always enhanced

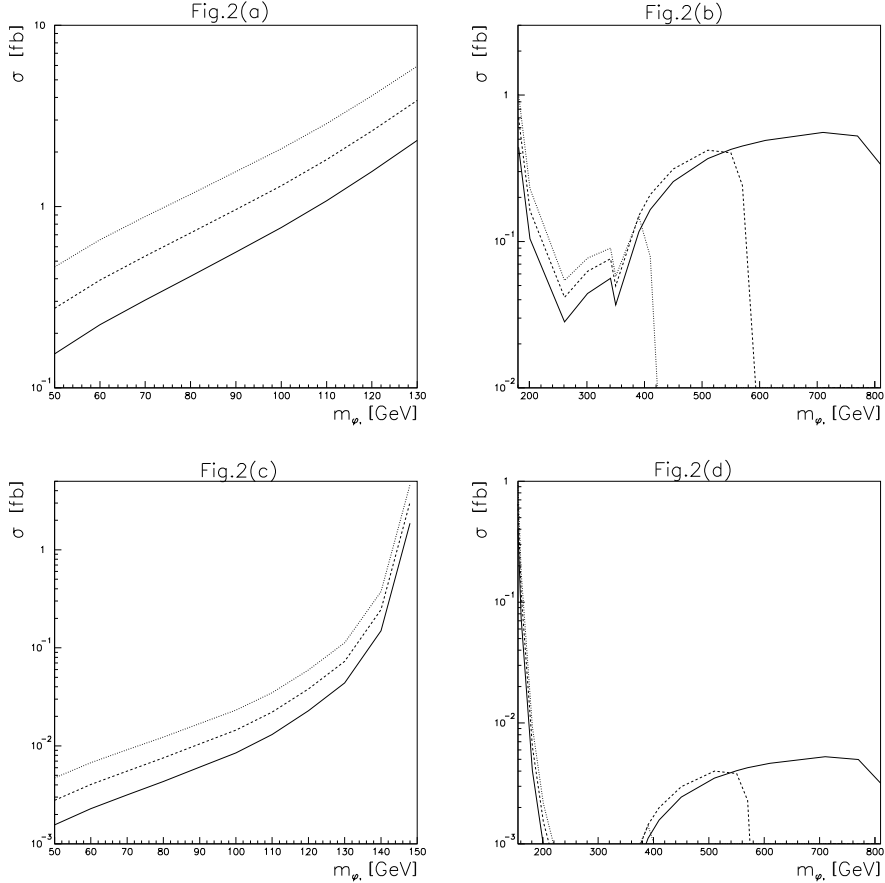


Figure 2: Cross section of $\gamma\gamma \rightarrow \phi'$ as a function of $m_{\phi'}$ with $m_h = 150$ GeV and $\xi = 1/6$. In (a) and (b) $\Lambda_\phi = 1$ TeV, and in (c) and (d) $\Lambda_\phi = 10$ TeV. The solid line corresponds to $E_{cm} = 1$ TeV, the dashed line to 700 GeV, and the dotted line 500 GeV.

due to mixing.

The cross section in the case of negative ξ is given in Figs. 4 (a) and (b), with $m_h = 150$ GeV and $\Lambda_\phi = 1$ TeV. Instead of suppression at heavy radions, there is a suppression for light radions and enhancement for heavy radions. This is reasonable because $a_{12} \sim \left(1 - \frac{6\xi m_\phi^2}{m_\phi^2 - m_h^2}\right)$ [10] when $\Lambda_\phi \gg v$. The gap in $m_{\phi'}$ for the region $m_{\phi'} \sim m_h$ is due to the same reason than in Fig. 2.

If the mixing of radion and Higgs is not very large and vacuum expectation value of radion is much larger than the VEV of Higgs, $\Lambda_\phi \gg v$, the mixing will effect Higgs considerably only when $m_\phi \sim m_h$, in which case a_{34} will be somewhat suppressed, as seen in Fig. 4 (a). When radion is clearly heavier or lighter than Higgs, a_{34} will be near one and Higgs coupling to fermions and massive gauge fields changes only slightly. However, this conclusion does not hold

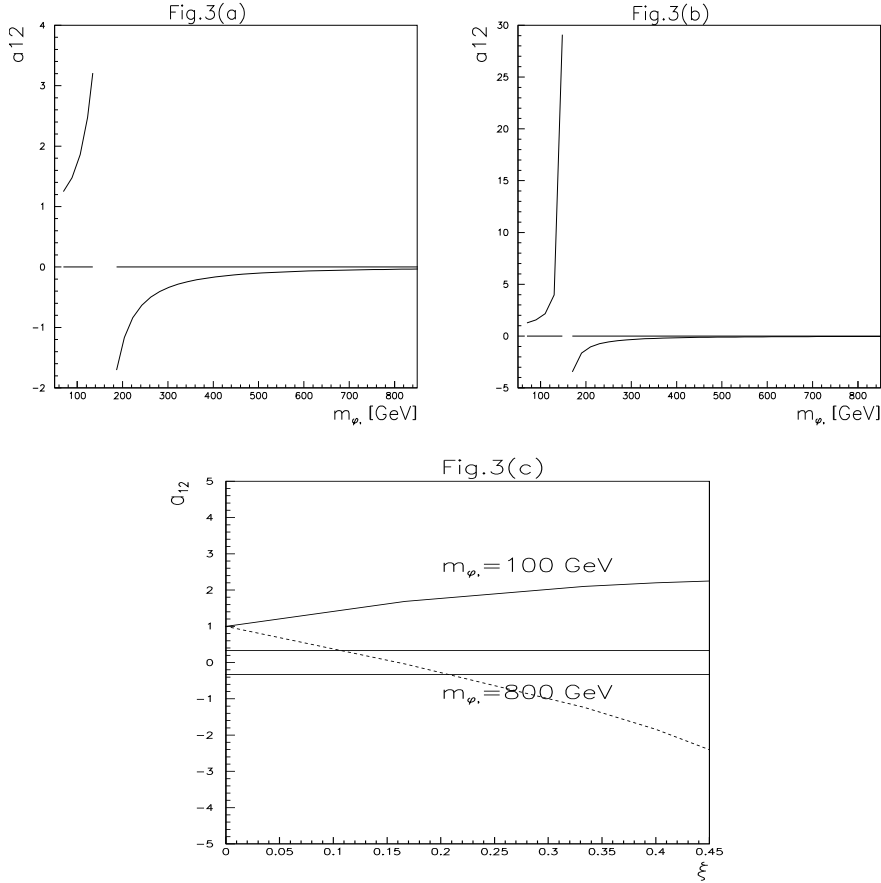


Figure 3: a_{12} as a function (a) of $m_{\phi'}$ with $\Lambda_\phi = 1$ TeV and $\xi = 1/6$, b) of $m_{\phi'}$ with $\Lambda_\phi = 10$ TeV and $\xi = 1/6$ and (c) of ξ with $\Lambda_\phi = 1$ TeV. Solid line corresponds to $m_{\phi'} = 100$ GeV and dashed line to $m_{\phi'} = 800$ GeV, and the horizontal lines correspond to ± 0.33 . In all cases $m_h = 150$ GeV.

when we consider the case $\Lambda_\phi \sim v$. In Fig. 4 (b) we draw a_{34} as a function of the radion mass with $\Lambda_\phi = 250$ GeV, $m_h = 150$ GeV, and $\xi = -1/6$. In this case the Higgs vacuum expectation value is of the same order than the radion, and mixing can effect Higgs strongly.

III. Radion decay

In order to detect the possible radion signal at LC, we consider the decay of radions in this section.

In Fig.6 (a), we give the branching ratio of radion in the no-mixing case, $\xi = 0$, with $m_h = 150$ GeV and $\Lambda_\phi = 1$ TeV. We find that our results disagree with the calculations in [8] and [10], but agree with those in [7]. The branching ratios for $\phi' \rightarrow gg$ and $\phi' \rightarrow b\bar{b}$ are both important

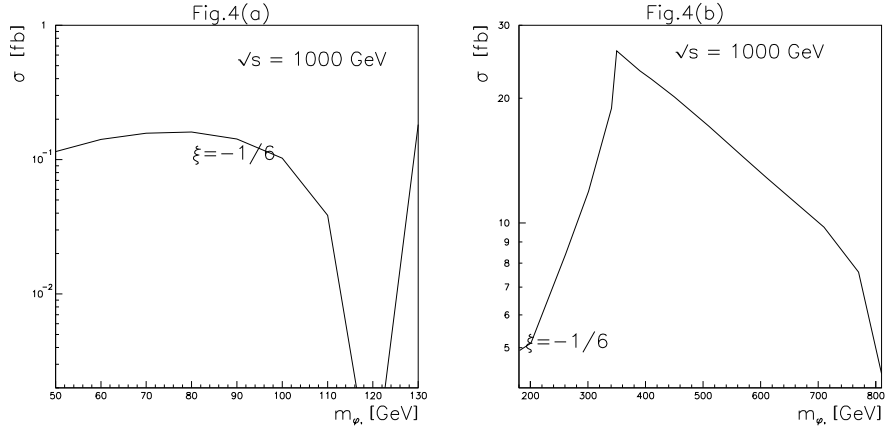


Figure 4: Cross section of $\gamma\gamma \rightarrow \phi'$ as a function of $m_{\phi'}$ with $\Lambda_\phi = 1$ TeV, $m_h = 150$ GeV, $\xi = -1/6$, and $E_{cm} = 1$ TeV.

for light radions (with mass below $2m_{W,Z}$). For heavy radions, WW, ZZ will dominate and distinguishing them from Higgs will be difficult.

In Fig. 6 (b) and (c), we plot the branching ratio of radion with $\xi = 1/6$, $m_h = 150$ GeV and $\Lambda_\phi = 1$ TeV, 10 TeV respectively. In this case, the decay of a heavy radion will be dominated by $\phi' \rightarrow gg$ and will be easily distinguished from Higgs, and a light radion will decay into $\phi' \rightarrow gg$ and $\phi' \rightarrow b\bar{b}$, with approximately the same branching ratios. Another interesting thing is that BR of $\phi' \rightarrow \gamma\gamma$ will increase with increasing the mass of a heavy radion.

IV. Conclusion

We have studied the process $\gamma\gamma \rightarrow \phi'$ in the RS model with curvature-Higgs mixing. The calculations show that radion production from $\gamma\gamma$ collision will be an important way to produce radion at LC and even a dominating way when the mixing parameter ξ is around the conformal limit.

Our calculations show that it should be possible to detect a radion for $E_{cm} = 1$ TeV with mass below 800 GeV if Λ_ϕ is around 1 TeV. Even if Λ_ϕ is about 10 TeV, the light radion with mass around m_h may be observable because of enhancements from mixing.

The decay modes of radion in the mixing case will be quite different from no-mixing case when radion is heavy or its mass is around m_h . Not only a light radion, but also a heavy radion will decay mainly to gluon-gluon, if mixing is around conformal limit. It can be clearly distinguished from the Higgs decay.

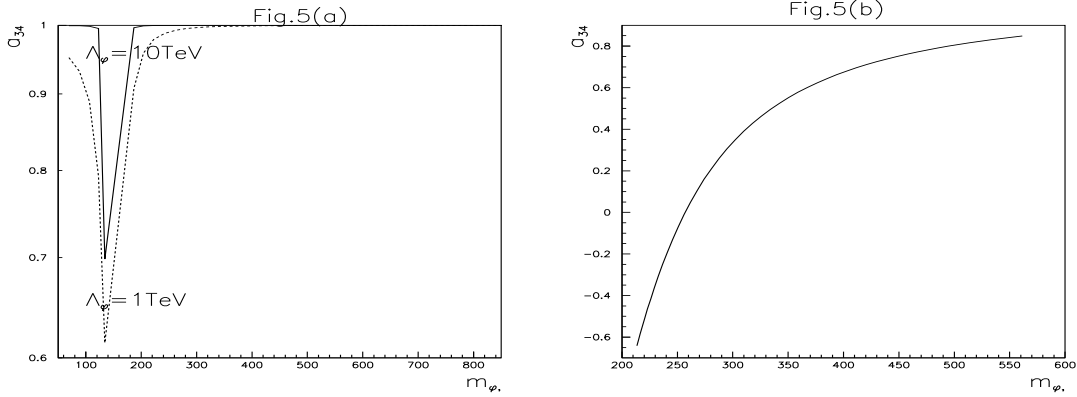


Figure 5: a_{34} as a function of $m_{\phi'}$ with $m_h = 150$ GeV and $\xi = 1/6$. (a) The solid line corresponds to $\Lambda_\phi = 10$ TeV and the dashed line to $\Lambda_\phi = 1$ TeV. (b) Here $\Lambda_\phi = 250$ GeV, $m_h = 150$ GeV and $\xi = 1/6$.

Acknowledgement

Z.-H. Yu thanks the World Laboratory, Lausanne, for the scholarship.

Appendix

A. Form factors

The form factors $F_{1/2}(\tau_t)$ and $F_1(\tau_W)$ can be defined as [10][15]

$$F_{1/2}(\tau) = -2\tau[1 + (1 - \tau)f(\tau)] \quad (A.2)$$

and

$$F_1(\tau) = 2 + 3\tau + 3\tau(2 - \tau)f(\tau) \quad (A.2)$$

where $\tau_t = 4m_t^2/q^2$, $\tau_W = 4m_W^2/q^2$ and

$$\begin{aligned} f(\tau) = & [\sin^{-1}(1/\sqrt{\tau})]^2, \quad \tau \geq 1, \\ & -1/4[\text{Log}(\eta_+/\eta_-) - i\pi]^2, \quad \tau < 1, \end{aligned} \quad (A.3)$$

with $\eta_{\pm} = 1 \pm \sqrt{1 - \tau}$.

B. $\gamma\gamma$ collision

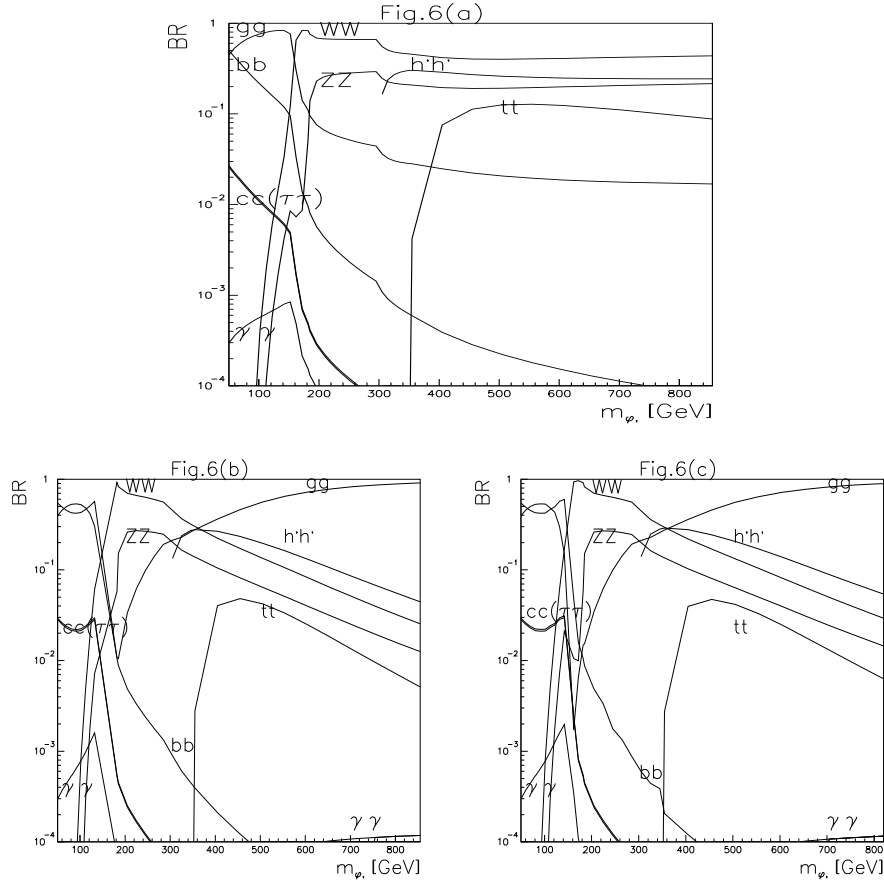


Figure 6: Branching ratio of radion as a function of $m_{\phi'}$ with (a) $\Lambda_\phi = 1$ TeV and $\xi = 0$. In (b) $\Lambda_\phi = 1$ TeV and $\xi = 1/6$ and in (c) $\Lambda_\phi = 10$ TeV and $\xi = 1/6$. In all cases $m_h = 150$ GeV.

In order to get the observable results in the measurements of radion production via $\gamma\gamma$ fusion in e^+e^- collider, we need to fold the cross section of $\gamma\gamma \rightarrow \phi'$ with the photon luminosity,

$$\sigma(s) = \int_{m_{\phi'}/\sqrt{s}}^{x_{max}} dz \frac{dL_{\gamma\gamma}}{dz} \hat{\sigma}(\hat{s}), \quad (B.1)$$

where $\hat{s} = z^2 s$, \sqrt{s} and $\sqrt{\hat{s}}$ are the e^+e^- and $\gamma\gamma$ c.m. energies respectively, and $\frac{dL_{\gamma\gamma}}{dz}$ is the photon luminosity, which is defined as [12]

$$\frac{dL_{\gamma\gamma}}{dz} = 2z \int_{z^2/x_{max}}^{x_{max}} \frac{dx}{x} F_{\gamma/e}(x) F_{\gamma/e}(z^2/x). \quad (B.2)$$

The energy spectrum of the back-scattered photon is given by [12].

$$F_{\gamma/e}(x) = \frac{1}{D(\xi)} \left[1 - x + \frac{1}{1-x} - \frac{4x}{\xi(1-x)} + \frac{4x^2}{\xi^2(1-x)^2} \right]. \quad (B.3)$$

taking the parameters of Ref. [16], we have $\xi = 4.8$, $x_{max} = 0.83$ and $D(\xi) = 1.8$.

References

- [1] N. Arkani-Hamed, S. Dimopoulos and G. Dvali, Phys. Lett. **B429** (1998) 263; N. Arkani-Hamed, S. Dimopoulos and G. Dvali, Phys. Lett. **B436** (1998) 257.
- [2] L. Randall and R. Sundrum, Phys. Rev. Lett. **83** (1999) 3370; L. Randall and R. Sundrum, Phys. Rev. Lett. **83** (1999) 4690.
- [3] W.D. Goldberger and M.B. Wise, Phys. Rev. Lett. **83** (1999) 4922; W.D. Goldberger and M.B. Wise, Phys. Rev. **D60** (1999) 107505.
- [4] M. Luty and R. Sundrum, Phys. Rev. **D62** (2000) 035008.
- [5] C. Csaki, M. Graesser, L. Randall and J. Terning, Phys. Rev. **D62** (2000) 045015.
- [6] W.D. Goldberger and M.B. Wise, Phys. Lett. **B475** (2000) 275.
- [7] U. Mahanta and S. Rakshit, Phys. Lett. **B480** (2000) 176; U. Mahanta and A. Datta, Phys. Lett. **B483** (2000) 196.
- [8] S. Bae, P. Ko, H.S. Lee and J. Lee, Phys. Lett. **B487** (2000) 299; S. Bae, and H.S. Lee, hep-ph/0011275.
- [9] K. Cheung, Phys. Rev. **D** 63 (2001) 056007, hep-ph/0009232; S.R. Choudhury, A.S. Cornell and G.C. Joshi, hep-ph/0012043.
- [10] G.F. Giudice, R. Rattazzi and J.D. Wells, Nucl. Phys. **B** 595 (2001) 250.
- [11] C. Csaki, M. Graesser and G. Kribs, Phys. Rev. **D63** (2001) 065002.
- [12] V. Telnov, Nucl. Instrum. Meth. **A294** (1990) 72; L. Ginzburg, G. Kotkin and H. Spiesberger, Fortschr. Phys. **34** (1986) 687.
- [13] G. Dvali, G. Gabadadze and M. Poratti, Phys. Lett. **B485** (2000) 208; H. Collins and B. Holdom, Phys. Rev. **D62** (2000) 124008.
- [14] R. Crewther, Phys. Rev. Lett. **28** (1972) 1421; M. Chanowitz and J. Ellis, Phys. Lett. **40B** (1972) 397; K.R. Dienes, E. Dudas and T. Gherghetta, Nucl. Phys. **B567** (2000) 111.
- [15] J.F. Gunion, H.E. Haber, G.L. Kane and S. Dawson, *The Higgs Hunter's Guide*, Addison-Wesley: Redwood City, California, 1989.
- [16] K. Cheung, Phys. Rev. **D47** (1993) 3750; ibid. 50 (1994) 1173.